Modeling Flashover of AC Outdoor Insulators under Contaminated Conditions with Dry Band Formation and Arcing

by

Lin Bo

A Thesis Presented in Partial Fulfillment
of the Requirements for the Degree
Master of Science

Approved February 2012 by the
Graduate Supervisory Committee:

Ravi Gorur, Chair
Vijay Vittal
Richard Farmer

ARIZONA STATE UNIVERSITY

May 2012

ABSTRACT

A power system can be well designed to withstand expected lightning and switching surge voltages with proper insulation coordination. However, when the insulator surface is covered by a pollution layer, flashover could happen at lower voltages. This has been a well known weakness of outdoor insulators [1, 2]. Various national and international standards organizations have developed standards to evaluate this aspect in the laboratory [3]. The tests are fairly elaborate and incur significant labor and cost. Good theoretical models for calculating the flashover voltage will enhance the value of the experiments and permit transmission line engineers to make reasonable predictions over a wide range of operating conditions and for insulators incorporating different shapes and materials. This report presents a theoretical model for evaluating the performance of insulators in terms of pollution severity at which flashover occurs for different system voltages and various insulator configurations and material types. The model introduces several new features such as, the formation of dry bands along the insulator surface and variations in surface wettability. The model draws heavily from experimental measurements of flashover voltage and surface resistance measured under varying wet conditions of insulators with housings made from silicone rubber, ethylene, propylene rubber and epoxy, as well as electric field distributions obtained from software for 3-dimensional models. It has been demonstrated that it is possible to change the insulator shapes without changing the leakage distance and realize significant improvement in flashover performance. The predictions have been validated with experimental results.

To
my parents Song Bai and Peiqin Xue
for their endless love and support

ACKNOWLEDGMENTS

I would like to express my sincere gratitude to my advisor Professor Ravi Gorur, whose expertise, understanding, and patience, added considerably to my graduate experience. He not only taught me about research, but also helped me to improve my writing, thinking and communication skills. He provided me with direction and support in the areas not only restricted to research but also in life and career, and became more of a mentor and friend.

Special thanks towards Professor Richard Farmer and Professor Vijay Vittal, whose kindness, care and encouragement have supported me continuously during my years at Arizona State University, which truly made a difference in my life. I appreciate a lot for their time and consideration in being on my supervisory committee. It is great honor to have them.

I am also grateful for the faculty of the power systems group at Arizona State University for their guidance and help throughout my graduate program. I must acknowledge all my friends from Arizona State University and Huazhong University of Science and Technology for their tremendous support over the years.

I would like to thank ABB Corporate Research, North Carolina, USA for their continued support and funding towards this project, and precious advice for this study.

Finally, I would like to extend my thanks to my family and my boyfriend, for always standing by me and shining me with endless love.

TABLE OF CONTENTS

CHAPTER Page

CHAPTER Page

LIST OF TABLES

LIST OF FIGURES

Figure Page

NOMENCLATURE

a	Arc constant 1
A	Arc constant 2
dl	The increment of integration.
E_c	Critical stress in V/mm
E_p	The voltage gradient of the pollution layer
F	A function of the product
$F\left(\frac{N}{A}\right)$	A function of the ratio of N and A
I	Leakage current
I_c	Critical current (A).
I_r	Peak value of leakage current in previous half cycle (A).
L	The leakage distance
$L\_electrode$	Length of the electrode
$L\_initial$	Length of the initial dry band
L_max	The maximum length of the dry band
L_{water}	Latent heat of vaporization water (2270J/g)
n	Arc reignition exponent
N	Arc reignition constant
$P(l)$	The circumference at partial creepage distance l
r_{pu}	Pollution resistance per unit length
$R_{insulator}$	Radius of the insulator
R_s	Internal resistance of the power supply

$R(x)$	The resistance from the grounding electrode to the arc root
V_a	Arc voltage
V_r	Reignition voltage (V peak)
W	Wetting rate (g/m^2/s)
X	Length of the arc
X_c	The critical length

CHAPTER 1

INTRODUCTION

The bulk of electric power is transmitted from generation sites to the distribution level through overhead transmission lines. These lines can span over thousands of kilometers. Towers are used to physically support the high voltage conductors. Insulators are widely used to support a conductor physically, and electrically separate it from other objects [4].

Historically, the transmission grid was designed based on existing power flows. Due to increasing demand for electrical energy, environmental concerns and state-lead initiatives to encourage renewable energy development, even higher system voltages for power transmission have to be used in order to reduce the power loss on the lines. Many countries have put a lot of efforts into the development of extra high voltage transmission lines. In the United States of America, Canada and Russia, systems with voltage over 750 kV have existed for many years. China has completed the construction of a 1000 kV AC system. Both India and China are planning to construct 1200 kV systems in the near future [5]. The higher voltage level would subject insulators to huge electric stress.

Besides the electric stress, insulators are subjected to a lot of other stresses [4]. Outdoor environmental conditions vary over a wide range. Temperature and moisture can greatly affect the performance of insulators. For instance, moisture like rain, dew, fog and melting ice significantly lower the surface resistance of insulators. With the presence of pollution, the insulator surface resistance is reduced even more. The reduction of surface resistance may cause increased

leakage current to flow on the surface and dry band arching to take place. Also, large magnitude leakage currents flowing on the surface for a long period may cause degradation of the insulator surface. With these factors, flashover may be initiated which leads to the failure of a line. In addition, temperature can affect the insulation properties of all material. For polymers that are organic materials, radiation from sunlight results in surface degradation. Altitude can also affect the insulator performance. Since air at ambient pressure and temperature is the primary insulation, higher altitudes reduce the air density, thus reducing the surface insulation strength.

Due to these factors, insulators must be well designed in order to work satisfactorily under a wide range of stresses. However, the construction of a transmission line needs a large number of insulators. Also, pollution levels vary with different areas. It would be a waste of money if the insulator is over designed. In order to improve the pollution flashover performance of insulators while reducing the cost of production, manufacturers seek optimal designs for insulators and conduct various experiments to verify the designs. Good theoretical models can help in quantifying the improvement during the design stage. This enhances the value of information obtained from laboratory experiments and field experience thereby helping transmission line engineers to make reasonable predictions and selections.

CHAPTER 2

BACKGROUND

2.1 Pollution flashover mechanism

For insulators energized with AC, the voltage distribution along the insulator under dry conditions is determined by the capacitance of the insulator and stray capacitances to the tower (ground). Under wet conditions, the voltage distribution is dominated by the surface resistance of the wet insulator, and is essentially linear prior to the initiation of dry band arcing [6, 7]. Even if the pollution layer is uniform, the presence of regions with different diameters on the insulator gives rise to different current densities. The narrow regions with higher current densities dry up first [7]. If several dry bands form, usually one will predominate and supply all of the voltage after a few seconds. The location of this dry band is usually near the energized end because of the higher electric field there. The width of the dry band changes until the electric field across it is equal to the electric field required to initiate a surface discharge. Most of the discharges across dry bands are extinguished, but occasionally one could grow to cause flashover [8, 9].

2.2 Types of insulators

The selection of insulators is mainly based on the voltage levels and environmental conditions. Insulators are classified largely by the dielectric material employed [4, 24]. The three main materials that are used for the manufacturing of insulators are polymer, glass and porcelain. Polymeric

insulators are also known as composite and nonceramic insulators. Porcelain insulators are also known as ceramic insulators. Porcelain and glass are dense materials; therefore insulators made from these materials are heavy. Due to the brittle nature of these materials, such insulators need to be handled carefully to avoid breakage. Porcelain and glass possess an extremely high resistance to heat and are not easily degraded. However, such materials are easily wettable by water. Hence insulators made from these materials need to have enough leakage distance and complicated shapes in order to retain a high surface resistance even in wet and contaminated environments. Composite insulators are lighter and are non-brittle. Therefore such insulators are easier to handle and install. The surface energy of composite materials is high and such insulators are not easily wetted. However, composite materials are more prone to deterioration by heat from arcs, chemicals and natural factors such as sunlight, temperature and moisture. With the passage of time, the electrical and mechanical properties of composite insulators can change. In other words, the insulator will “age”. Hence, the resistance to cracking and erosion of materials is an extremely important aspect of composite insulators. All materials undergo aging. It is more common to talk about aging with composite insulators； however，porcelain and glass insulators are also subject to aging, at a much slower rate [4].

2.3 Types of pollutants

There are various types of contaminants. The level and the type of pollution for a region are associated with the sources of pollution, and with climate of the

location [10]. For example, insulators in coastal areas usually encounter sodium chloride, while in inland areas, the pollutants are usually fly-ash, cement dust and paper pulp. During the winter in cold climates, salt is often used for de-icing streets, which could also become a source of pollutants [11]. Climate can play an important role in the pollution procedure. It might affect the pollution deposition and distribution on the insulator's surface, the durability of the pollution condition, and the pollution dispersion amount from resource. In general, pollution can usually be divided into three types: industrial, marine and desert [10].

2.3.1 Industrial pollution

In daily work, people and industry generate smoke, dust and other particles into the air. Wind spreads these particles over the areas where electric lines exist. The development of industry has resulted in large amount of particles emitted into the air. For example, for industries that consume fossil fuels and coal, the heavy particles of the fuel remain in suspension in the air. Heavy industries such as fertilizing plants and cement factories can also have severe emissions of contaminant particles. The particles slowly form a contamination layer on the insulator during a period that can last for months or years. By tracking the amplitude of the leakage current with respect to time, it is possible to see whether the activity of the pollution increases with time as well as the effect of the natural wash (rain). Thereby the necessity for artificial cleaning (maintenance) can be determined [10].

2.3.2 Marine pollution

In the morning, salted dew will be formed on the insulators in the zones close to the coasts. The evaporated salt will be deposited on the insulators when the dew is dried by ambient temperature or by the heat produced in the insulator. When the layer is dry, those particles are not dangerous. Problems arise when the atmosphere is humid and the layer can become conductive. The weather conditions vary considerably from the coastal areas to the inland. This type of pollution depends mainly on the environment [10].

2.3.3 Desert pollution

In the zones close to the desert, the insulators are often subject to the deposition of contaminant substances of the deserts. The pollution particles in this zone type are: the sand and the salty dust in a dry atmosphere. Sand storms and cyclones which are very common in the desert move the particles at a high speed. The high speed particles strike the surface of the insulators, causing material erosion. Thus, ceramic insulators have better performance than composite insulators in the desert. It needs to be noted that although the weather of deserts can sufficiently keep the insulator surface dry, the little quantity of rain results in very little natural washing. Therefore, when the pollution layer is dampened by the rain or dew, it could become very conductive. Areas with large current density can be easily heated, creating dry bands [10].

2.4 Levels of pollution (ESDD)

The severity of pollution in a location is quantified in terms of the Equivalent Salt Deposit Density (ESDD). The ESDD value provides a classification of the pollution severity in the zone, considers the weather factors like temperature, humidity, pressure, rain and wind velocity. It also helps determine the necessity of insulator maintenance. The highest ESDD value that an insulator can handle without flashover under a certain voltage level is an important characteristic considered by transmission line builders when choosing the proper insulators regarding the pollution level of the area. Different pollution levels and corresponding ESDD values are shown in Table 1 [12].

Table 1.Pollution levels and corresponding ESDD values (mg/cm^2)

Natural pollution levels	Salt Deposit Density, mg/cm^2
No significant pollution	0.0075 – 0.0150
Very light pollution	0.0150 – 0.0300
Light pollution	0.0300 – 0.0600
Average pollution	0.0600 – 0.1200
Heavy pollution	0.1200 – 0.2400
Very heavy pollution	0.2400 – 0.4800
Exceptional pollution	$\geq$0.48

2.5 Methods to enhance insulator performance

There are many ways to enhance insulator performance. One possibility is to increase leakage distance. This can be achieved by increasing the number of units,

using taller posts, sheds with ribs, alternating diameter sheds and creepage extenders [4]. Some recent studies show that by using an alternating diameter shed design or cup shed design, the insulator performs better than the commonly used straight designs in areas that are prone to dry band activity [11]. In fairly benign locations, surface hydrophobicity can be taken advantage of by enabling the use of silicone rubber (and other similar materials) insulators that have a lower leakage distance [4]. The methods include coating the insulator with room temperature vulcanized silicon rubber (RTV coating), covering the insulator with semi-conducting glaze and greasing the insulator with thin layer of petroleum grease. The problem with composite materials is that they are hydrophobic when they are new; this property diminishes with time in service. In order to enhance the time for which the surface is hydrophobic, there have been attempts to blend silicone polymers into EP rubber and epoxy [4]. Besides the design and material factors, periodic cleanings with high pressure water or high pressure driven abrasive materials are also very important for insulator maintenance.

CHAPTER 3

LITERATURE REVIEW ON FLASHOVER MODELS

3.1 Introduction

Hundreds of papers have been written in the last 70 years dealing with the subject of flashover models. Many researchers have worked to make a lot of useful contributions to this subject [13]. In the following chapter, a comprehensive summary is given for the development of flashover models. It is noted that, more or less, large amount of recent publications are based on the early models. A lot of researchers attempt to improve on the correlation between the predictions of their models and experiment results [2].

3.2 DC models

3.2.1 Mathematic representation of DC arc

Obenaus was the first to provide the analysis of the pollution flashover phenomenon [2]. The work modeled the flashover process as a discharge in series with a resistance.

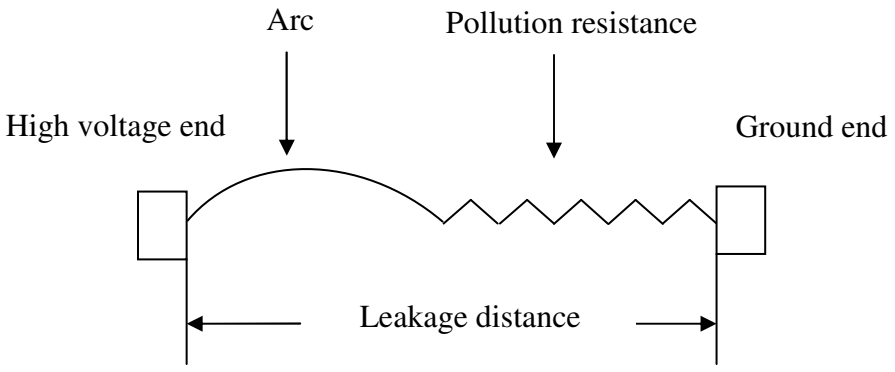

Figure 1.Basic model of Obenaus

The arc is represented by a voltage-current relationship represented by the equation below:

$$V_a = AXI^{-a} \tag{1}$$

Where:

V_a: arc voltage

A, a: arc constants

X: length of the arc.

The equation for the whole circuit is then:

$$V_s = V_a + R(x)I \tag{2}$$

Where:

I: the leakage current

$R(x)$: the resistance from the grounding electrode to the arc root.

For a cylinder shaped insulator with uniform pollution, there is a linear *R-X* relationship [2].

$$R(x) = r_{pu}(L - X) \tag{3}$$

Where,

r_{pu}: the pollution resistance per unit length.

L: the leakage distance

Alston further analyzed the relationship of the variables, and the work arrived at the relationship for the critical electric field leading to flashover [14]:

$$E_c = A^{\frac{1}{a+1}} r_{pu}{}^{\frac{a}{a+1}} \tag{4}$$

By multiplying E_c with L, the critical value of the supply voltage is obtained. The corresponding critical current is:

$$I_c = \left(\frac{A}{r_{pu}} \right)^{\frac{1}{a+1}} \tag{5}$$

The flashover will occur at arc length:

$$X_c = \frac{L}{a+1} \tag{6}$$

From equation (4) and (5) it can be seen that:

$$E_c I_c{}^a = A \tag{7}$$

Alston also determined the arc constants of *A=6.3* and *a=0.76* from experimental data [14].

3.2.2 Arc propagation criteria

Based on flashover experiments on a uniform water column, Hampton established the necessary condition for arc propagation [15]. That is, the arc will propagate if the voltage gradient of the pollution layer is greater than that of arc gradient. This means that the ionization of the path ahead of the arc by the increasing current at every instant enables the arc to proceed.

$$E_a < E_p \tag{8}$$

Hesketh derived a general formula for this criterion, that for a power supply with an internal resistance R_s, the flashover criterion takes the form [16]:

$$\frac{E_a + i\dfrac{dR(x)}{dx}}{x\dfrac{dE_a}{di} + R(x) + R_s} < 0 \qquad (9)$$

Rizk has shown that the criterion derived by Heskesh gives the same results as the criterion developed by Hampton. With arc constant *A=6.3* and *a=0.76*, the prediction thus gives the same satisfactory results [17, 2].

In 1993, Sundararajan developed a model to estimate the pollution flashover voltage for various insulators using Hampton's criterion together with a dynamic arc characteristic.

3.3 AC models

3.3.1 DC models applied to AC

The sinusoidal AC voltage wave is almost flat near the peak value. With the peak value used, the DC equation can also apply. However it was found that, with the same value for constants *A* and *a* used in the DC model, the prediction results were lower than the measured AC results [2]. Many researchers have chosen different constants in the AC models in order to fit their experimental data [2]. For example, when Woodson used Alston's method for a circular disc energized in AC, he choose *A=200* instead of *6.3* [18, 2].

Rizk pointed out that the phenomenon of AC flashover is quite different when the flashover time is no longer than the duration of half a wave of the supply voltage. He further showed that, although AC and DC equations have

similar forms, it is possible to fit both equations to experimental data, but the values of the constants are different for two types of energizations [2, 17, 19].

3.3.2 AC reignition models

Claverie was the first to point out the role of arc reignition [20, 21, 2]. He obtained the relationship for the minimum voltage supply that is needed to ensure reignition of an AC arc from the previous half cycle.

$$V_r = NXI_r^{-n} \tag{10}$$

Where:

V_r: reignition voltage (V peak)

N: arc reignition constant

n: arc reignition exponent

X: arc length (mm)

I_r: peak value of leakage current in previous half cycle (A).

It is noted that equation (10) is similar to equation (1). With $a=n$ and $I=I_r$, combining the DC and Arc equation, the following relationships are obtained [2]:

$$E_c = \frac{N}{L}\left(N - A\right)^{-\frac{n}{n+1}} X_c^{\frac{1}{n+1}} R\left(x\right)^{\frac{n}{n+1}} \tag{11}$$

$$I_c = \left(\frac{NX_c}{LE_c}\right)^{\frac{1}{n}} \tag{12}$$

Where:

X_c: the critical length

E_c: critical stress in V/mm

I_c: critical current (A).

For a uniform pollution layer, it was shown that:

$$X_c = \frac{L}{n+1} \tag{13}$$

With X_c substituted in to equation (11), it is seen that [2]:

$$E_c = \frac{1}{n+1} N(N-A)^{-\frac{n}{n+1}} n^{\frac{n}{n+1}} r_{pu}^{\frac{n}{n+1}} \tag{14}$$

Where

E_c: critical stress (V/mm)

L: leakage length of the insulator (mm)

r_{pu}: average pollution resistance per unit length (ohm/mm).

With X_c substituted into (12):

$$I_c = \left(\frac{N}{(n+1)E_c} \right)^{\frac{1}{n}} \tag{15}$$

Equation (15) can also be written in the form of:

$$E_c I_c^{\,n} = \frac{N}{n+1} \tag{16}$$

This is quite similar to the "DC" counterpart, equation (7) [2].

3.3.3 Dimensional analysis

In 1970, Rizk [19] pointed out a special way to analyze the process of pollution flashover also known as dimensional analysis. According to the method, the relationship among a complete set of dimensionless products can be converted to a dimensionally homogenous equation. Rizk showed that by using dimensional

analysis, he could obtain most of the equations derived by early researchers. The equation for AC flashover is:

$$E_c = F \cdot \left(r_{pu}^{\left(\frac{a}{a+1}\cdot\frac{n}{n+1}\right)} \cdot N^{\frac{-1}{n+1}} \right) \cdot A^{\frac{1}{a+1}} \cdot r_{pu}^{\frac{a}{a+1}} \tag{18}$$

Where: F denotes a function of the product.

For the case $a=n$, the equation becomes:

$$E_c = F_1 \cdot \left(\frac{N}{A}\right) \cdot r_{pu}^{\frac{n}{n+1}} \cdot N^{\frac{1}{n+1}} \tag{19}$$

Where:

$F\left(\frac{N}{A}\right)$: denotes a function of the ratio of N and A.

It is noted that equation (19) is quite similar with equation (7) [2].

CHAPTER 4

DESCRIPTION OF THE NEW MODEL

4.1 Problems in existing models

As seen from the literature review, after the formation of the dominant dry band, further propagation depends on whether the voltage gradient of the pollution layer is greater than that of arc gradient ($E_p > E_{arc}$) [6]. This ensures that the increasing current is able to sustain ionization of the path ahead of the arc and enables it to proceed. This criterion is widely used in the existing flashover models.

The electric field for arc and pollution layer is calculated using the following equations.

$$E_{arc} = NI^{-n} \tag{20}$$

$$E_p = r_{pu} I \tag{21}$$

Where:

N : reignition constant

n: reignition exponent.

By increasing the supply voltage or pollution severity, the leakage current will increase to a level so that E_{arc} is smaller than E_p. The current further increases as the arc starts to propagate on the surface. From the equations, it can be seen that E_{arc} will decrease and E_p will increase. Once E_{arc} is smaller than E_p, it will remain so as long as the current is increasing. That means once the arc starts to propagate, it cannot stop until flashover occurs.

In reality, when voltage is applied on wet and contaminated insulators, the current will cause Ohmic heating to form a dry band [6]. If the dry band length is sufficiently long, the current will decrease and the arc is extinguished. Another scenario for arc extinction is if the polluted surface is hydrophobic, the current will then be too small to establish a dry band [22].

Thus, in order to better simulate the flashover process, new criteria must be introduced. In the proposed model, a new criterion is introduced to check if a dry band can be formed and if the arc is able to bridge the dry band in order to continue propagation.

4.2 Simulation process in the new model

In the model presented in this paper, the flashover progress is modeled mainly in three stages: (1) The formation of "initial arc"; (2) Arc propagation on surface. (E_{arc}<E_p); (3) Dry band formation and arc bridging.

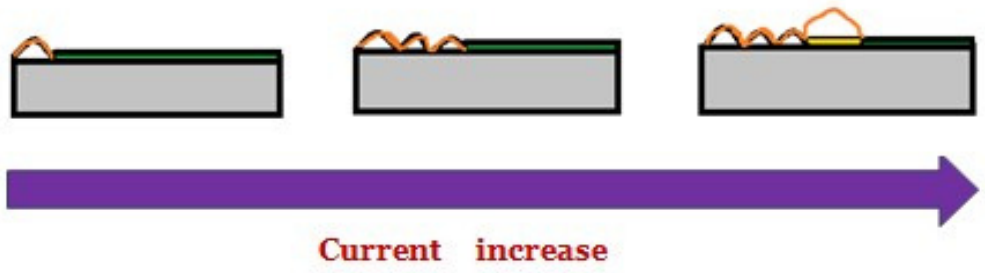

Figure 2.The simulation process

4.2.1 The formation of initial dry band

The proposed algorithm starts with the calculation of the pollution resistance considering the initial condition without any arc. Form factor is used to calculate

the resistance of the insulator. It takes into consideration the effect of the shape of the insulators, and is calculated from the data of insulator geometry. The pollution resistance *R* is determined from the following equation [3]:

$$R = \frac{1}{layer\_conductivity} \cdot form\_factor \tag{22}$$

$$form\_factor = \int_0^L \left[\frac{1}{p(l)} \right] dl \tag{23}$$

Where :

L: the total creepage distance

P(l): the circumference at partial creepage distance *l*

dl: the increment of integration.

The pollution resistance is then used to calculate the leakage current, which will be used to determine if dry bands can form. The power dissipated in the pollution layer due to ohmic heating goes against the rate of moisture deposition on the polluted surface [23]. The ohmic heating is the source of energy dissipation needed for evaporation.

The power dissipation per square meter (W/m^2) is:

$$P_w = \frac{E \cdot I}{2 \cdot \pi \cdot R_{insulator}} \tag{24}$$

Where:

$\frac{I}{2 \cdot \pi \cdot R}$: the current density

$R_{insulator}$: the radius of the insulator.

The power per square meter necessary to evaporate a unit mass of water (W/m^2) is:

$$P_e = L_{water} \cdot W \tag{25}$$

Where

L_{water}: latent heat of vaporization water (2270J/g) [23]

W: Wetting rate ($g/m^2/s$).

For a dry band to form, the evaporation rate must be higher than the wetting rate. In that case, the current should be big enough to start forming a dry band [23]. If dry bands do not form, the algorithm will increase the conductivity of the contamination until the current is big enough to start evaporating water.

The length of the initial dry band will then be calculated using the electric field required to initiate a discharge in the air [9]. Based on the literature review, the non uniform field value varies from 4.5 to 11 kV/cm [25]. A value of 6 kV/cm has been used in the model. The maximum length of the dry band on which the electrical field is high enough to cause arc jumping in the air is:

$$L\_max = \frac{V_{\sup ply}}{6kV} \tag{26}$$

The location of the initial dry band is usually on the narrow part (shank of the insulator) near the high voltage electrode. Some insulators may have a shed very close to the hardware, in which case, the thin part will dry out much quicker than the shed and the dry band length is smaller than previously suggested. The program will compare the length of the electrode (*L_electrode*) and *L_max*, and determine the length of the initial dry band (*L_initial)* as follows:

If *L_max >= L_electrode*, *L_initial =L_electrode*.

If *L_max<L_electrode, L_intial = L_max*.

After the formation of the initial dry band, an initial arc is assumed to occur and bridge the dry band. The program will check the leakage current with the dry band bridged by the arc. If the resulting current is not able to sustain the arc, the arc will become unstable and extinguish [6]. Based on the literature, the minimum value of current for sustaining the arc is in the range of 2 -8 mA [6].

4.2.2 Arc propagation on the surface of insulator

The program will continue to check if E_{arc} is smaller than E_p to see if an arc can start propagating on the insulator surface. If E_p is bigger than E_{arc}, the arc is able to propagate. The program will continue to check for further dry band formation and arc bridging. If not, the program will increase the conductivity of the pollution layer thus increasing the leakage current until E_p is bigger than $E_{arc.}$

4.2.3 Further dry band formation and arc bridging

As the arc propagates on the surface, the leakage current will increase. The electric field distribution on the surface is used to determine the power dissipation. The power dissipation is further used to determine the dry band length. The voltage distribution on a contaminated surface varies from the capacitive distribution, on a dry surface, to a resistive one on a uniformly wet surface [27, 28].

The voltage distribution was determined by a 3-dimensional software package called “Coulomb” [29]. A 25 kV class (15 kV line to ground) standard post type porcelain insulator, shown in Figure 3, was modeled under both dry and wet conditions. For the wet case, the simulation was performed with a 1mm thickness water layer having conductivity of about 5μs/cm, which is close to that of rain water.

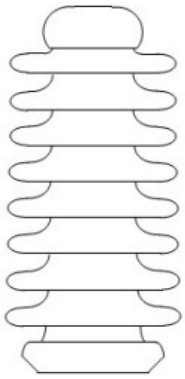

Figure 3.Schematics of the 25 kV class standard post type insulator

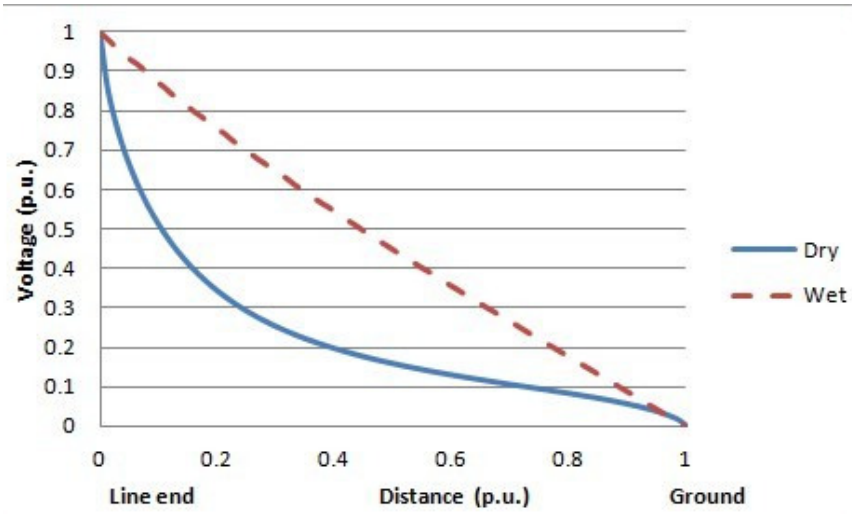

Figure 4.Voltage distribution on a contaminated post type insulator under dry and wet conditions (data obtained from Coulomb simulation)

A distribution midway between these two extremes was used. An equation was generated to fit the voltage distribution by the program Origin®. By taking the derivative of the equation, the expression for the surface electric field distribution was obtained and is shown in Figure 5.

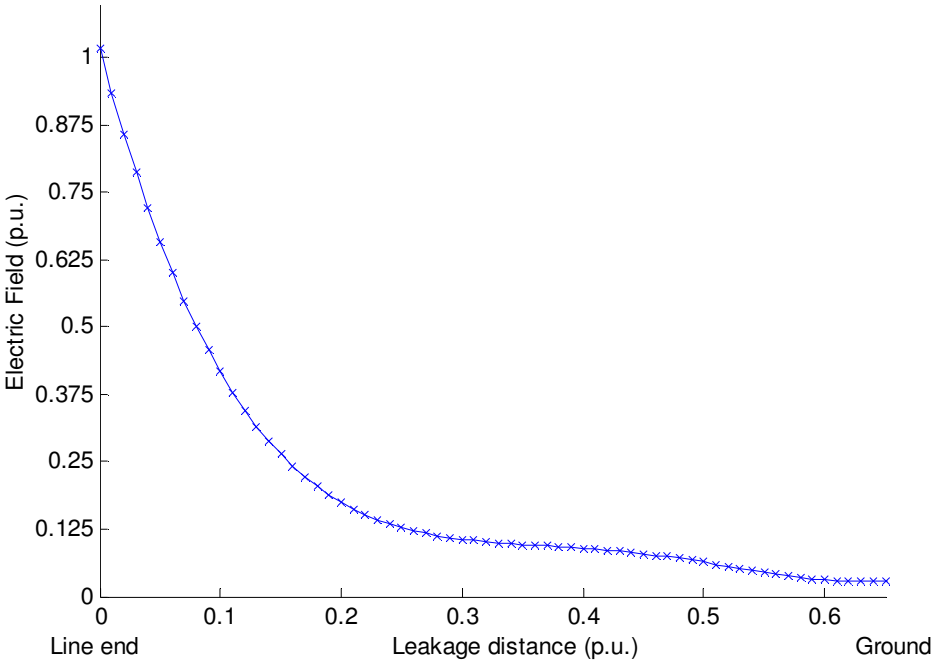

Figure 5.Illustrated electric field distribution on a contaminated post type insulator

As an example, let us assume that there is a certain thickness of water on the insulator. The amount of water that can be evaporated in a given time interval is calculated from the electric field distribution, wetting rate, leakage current, insulator (primarily the shank or narrow part) diameter and the latent heat value using equation (24) and (25). If this exceeds the assumed thickness, then a dry band is formed. Using the proposed method, the length of the dry band can be calculated. The time interval value used in the program is in the range of 1 to 7

minutes and is obtained from the clean-fog flashover experiments. The time is dependent on the wetting rate, contamination severity and insulator geometry. For example, with higher wetting rate, it takes longer for the dry band to be formed.

The program will use the supply voltage to check if the dry band can be bridged. If the dry band cannot be bridged (this happens on insulators with large shed spacing), the program introduces another criteria that will increase conductivity of the pollution until the leakage current reaches 8mA. In real life, usually the pollution layer and water film cannot be perfectly uniform, thus with a large enough current, it can quickly dry out the area with a thin water film and form a small dry band. Due to the high electric field concentration on the dry band, if the electric field on the dry band is adequate it will be quickly bridged by the arc. In other words, the dry band will not be slowly formed, and there will not be a long dry band on the insulator surface.

4.2.4 Conversion from conductivity to ESDD

The relationship of ESDD and layer conductivity is different for materials with different wettabilities. For example, for the same ESDD, the surface resistance values are much lower for hydrophilic materials like porcelain, EPDM and epoxy than silicone rubber whose surface is hydrophibic [30]. Experiments were conducted to investigate the relationship between the ESDD and surface resistance, in a fog chamber using conditions specified by the IEEE Task Force on surface resistance measurements [31, 26].The results were used to convert

conductivity to ESDD in the program. The measurement was conducted on three types of insulators, whose details are shown in Table 2.

Table 2.Details of insulators used for surface resistance &ESDD measurement

Material type	Leakage distance (cm)	Shed diameter (cm)	Shed spacing (cm)	Shank diameter (cm)
Silicone rubber	27.0	9.0	3.0	3.0
EPDM	26.0	9.0	2.0	2.0
Porcelain	20	15.5	1.2	4.5

Figure 6 shows the schematic of different samples tested in the fog chamber

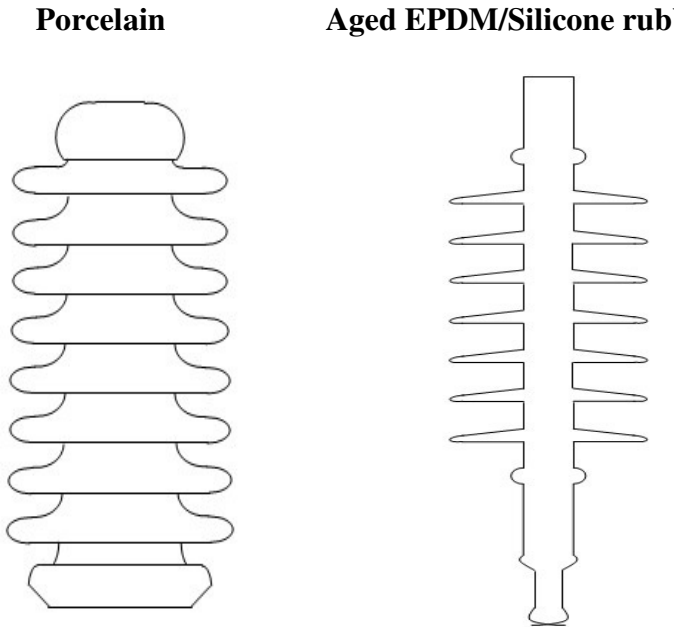

Figure 6.Schematics of the three insulators

The silicone rubber and EPDM samples were obtained as new samples and after 5 years of exposure in the field (near Chicago, USA). A porcelain line post

insulator was chosen for reference. The average diameter of the porcelain insulator is bigger than the composite insulators. The aged silicone rubber samples were still hydrophobic but EPDM samples had lost their hydrophobicity. The measured ESDD and corresponding surface resistance value is found in the reference paper [3, 12].

Table 3.Experimental measurements of surface resistance vs. ESDD for different materials

Material	R_{pu} (Mohm/cm)	ESDD (mg/cm^2)
EPDM	0.29	0.175
	0.22	0.185
	0.15	0.255
	0.125	0.275
Silicone Rubber	0.77	0.175
	0.65	0.185
	0.58	0.255
	0.46	0.275
Porcelain	0.5	0.1
	0.046	0.3

The pollution resistance can be calculated using equation:

$$R = L \times r_{pu} \tag{27}$$

L is the leakage distance; r_{pu} is the pollution resistance per unit length. As mentioned before, for a certain L, the pollution resistance:

$$R = \left(\frac{1}{layer\_conductivity} \right) \cdot form\_factor \tag{28}$$

Using the program to calculate the form factor for the measured insulator section with given geometry, the layer conductivity can be calculated:

$$layer\_conductivity = \frac{form\_factor}{L \cdot r_{pu}} \tag{29}$$

As it is known, there is a linear relationship between ESDD and layer conductivity [3]. A curve for the best fit of the measurement data was obtained to get the relationship between ESDD and conductivity.

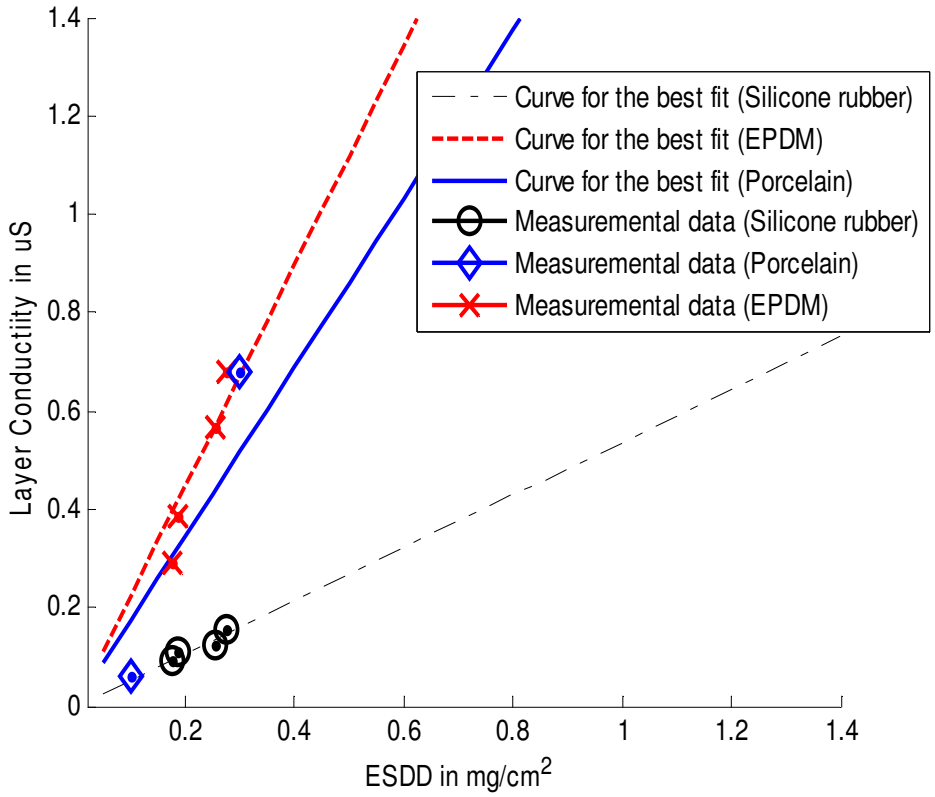

Figure 7: Correlation of ESDD with layer conductivity.

The fitted curve is used in the program to convert layer conductivity into ESDD, which is the final output result.

4.3 Program description

4.3.1 Program structure

The program was coded in Matlab (version 7.9.0). It calculates the pollution severity at which flashover occurs for a given system voltage. The program requires the user to define the insulator geometry, insulator material and the supply voltage. Running the program returns the ESDD value that causes flashover for the defined insulator and voltage. It will also plot a figure showing the results. The constants of $N= 34$ and $n= 0.33$ are used in the electric stress equation ($E_a= NI^n$). The model is applicable for an insulator energized with AC voltage as all experimental data has been obtained with AC voltage.

Table 4.Required inputs to define the insulator geometry

Number of small /big sheds	Big_Shed_Diameter	Small_Shed_Diameter
Shank_Diameter	Top_Diameter	Bottom_Diameter
Small_Shed_Thickness	Big_Shed_Thickness	Bottom_length
Top_Length	Big_Spacing	Small_Spacing
Big_Shed_Angle	Small_Shed_Angle	Bottom_Shank_Angle

4.3.2 Program flow chart

The flow chart of the program is shown in Figure 8. The program consisted of about 800 lines of code. The simulation process contains some integration calculations to dynamically check the change of resistance as the arc propagates. The computation time (on a personal computer with 4.00 GB memory and Intel®

Pentium® P6100 CPU) varied from 5-15 minutes depending on the size of the insulator modeled and the simulation step length.

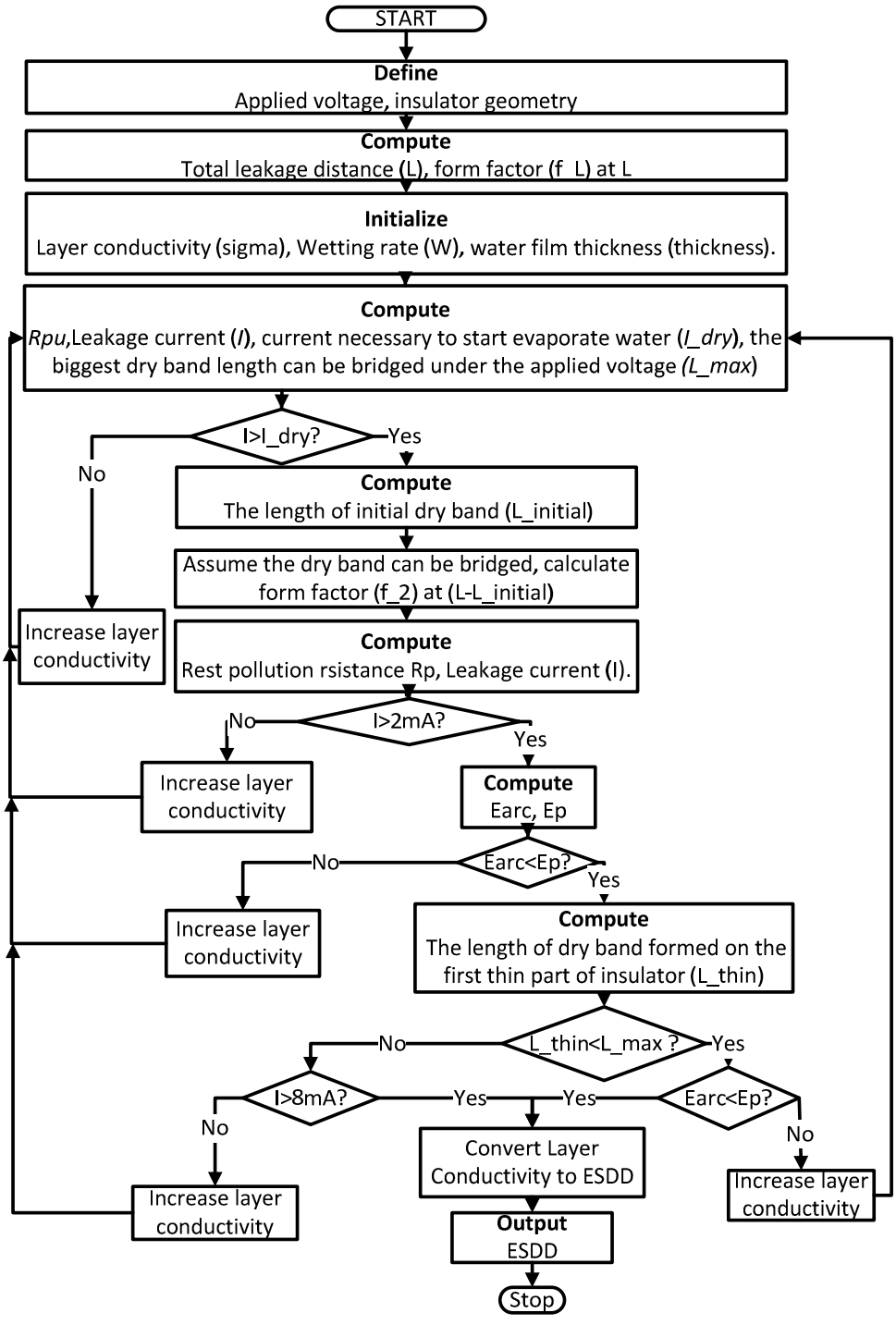

Figure 8.The program flow chart

CHAPTER 5

SIMULATION RESULTS AND DISCUSSTION

5.1 Role of active & non-active material

Housing materials can be classified as “active” or “inert”. Materials that retain and recover their hydrophobicity for a long time, such as silicone rubber, belong to the active category. Other polymer families such as EPDM and epoxy, and porcelain belong to the inert (or passive) category. For the same ESDD, the surface resistance values are much lower for inert material than for active materials [31].

Table 5 shows the measured surface resistance under wet conditions for different levels of ESDD. For the same ESDD value, the resistance of silicone rubber is roughly 3.5 times of EPDM.

Table 5.Surface resistance and ESDD measurements of EPDM and Silicone Rubber [31]

Material	r_{pu} (Mohm/cm)	ESDD (mg/cm^2)
EPDM	0.29	0.175
	0.22	0.185
	0.15	0.255
	0.125	0.275
Silicone Rubber	0.77	0.175
	0.65	0.185
	0.58	0.255
	0.46	0.275

5.1.1 Post type insulator with three housing materials

Simulation was performed for the 25 kV class (15 kV line to ground) standard post type porcelain insulator (Figure 9).

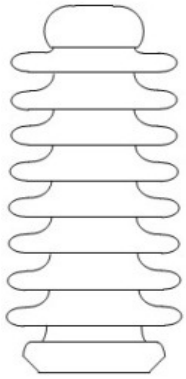

Figure 9.Post type insulator

The main geometry information of the insulator is shown in Table 6.

Table 6.Geometry information of the post type insulator

Insulator type	Post Type
Leakage distance	77cm
Shank diameter	4.5 cm
Big shed diameter	12 cm
Small shed diameter	8.6 cm
Standard Voltage (L-G)	15 kV

Figure 10 shows the relation between the flashover pollution severity and the applied voltage while varying the material of the insulator.

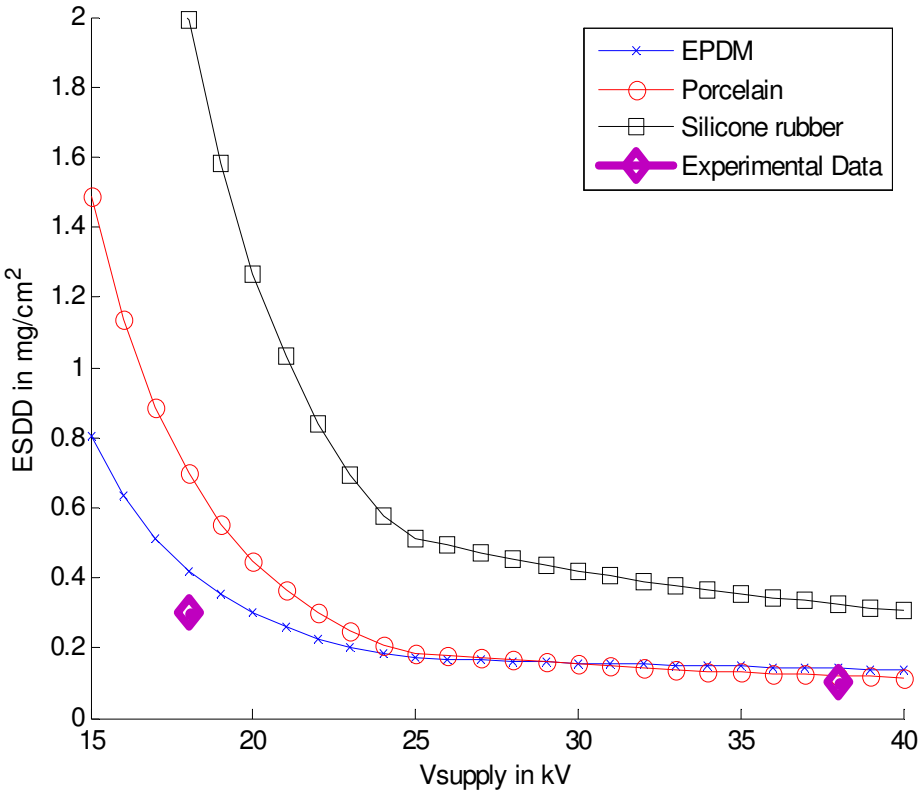

Figure 10.Simulation results for post type insulators with different materials

The simulation results for porcelain and EPDM show good agreement with the experimental data. The figure also shows the predicted ESDD value for flashover is much higher if the insulator material is changed from EPDM to silicone rubber.

5.1.2 Prediction of the performance of various materials

For the purpose of predicting the performance of materials with varying degrees of hydrophobicity, the calculations have been performed for materials with resistance values that are 1.5, 2 and 2.5 times the resistance of EPDM. The surface resistances under wet conditions for different levels of ESDD of these materials are shown in Figure 11.

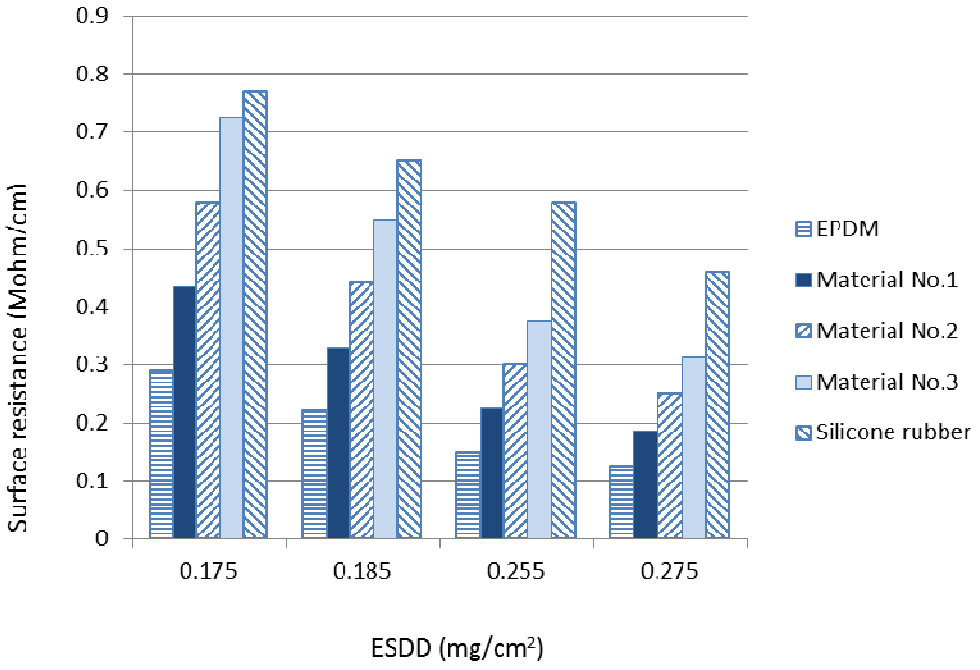

Figure 11.Surface resistances under wet conditions for different levels of ESDD of different materials

The simulation was conducted on a post type insulator with similar shape as shown in Figure 9. The dimensional details of the insulators modeled are shown in Table 7.

Table 7.Details of the post type insulator

Leakage distance (cm)	Big shed diameter (cm)	Small shed diameter (cm)	Shed spacing (cm)	Core shaft diameter (cm)
77	15.5	15.5	1.2	6.8

Figure 12 shows the flashover performance for insulators with identical geometry but with housing materials made from different materials.

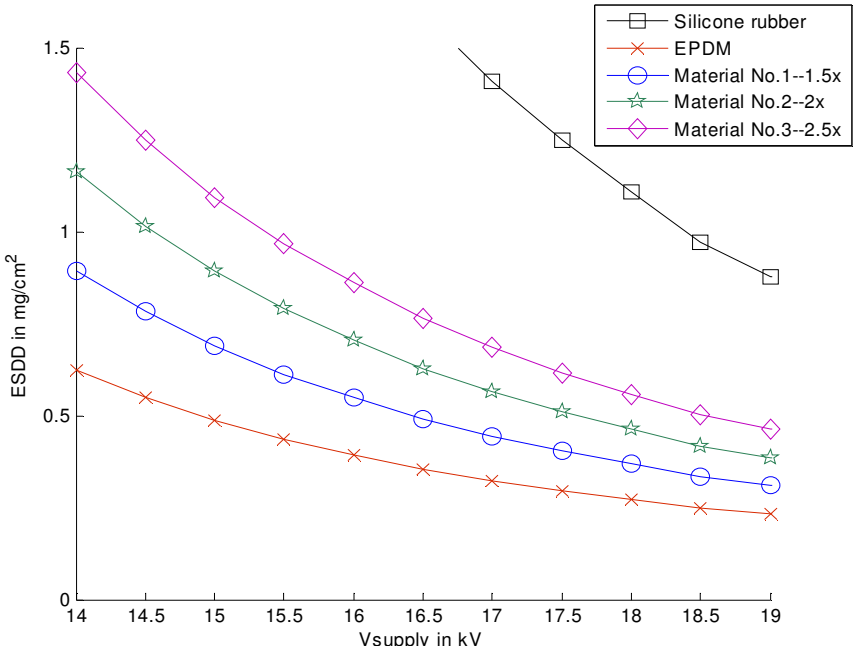

Figure 12.Simulation results for post type insulator with varying materials

This method can possibly be used in industry for insulator material selection. If an insulator manufacturing company wants to know whether a specific material can be used for a specific design of insulator, it can employ the above method using the flowing steps:

Step 1: Obtain the relationship between ESDD and conductivity for the specific material including:

A. Conduct the experiments to measure the ESDD and surface resistance value for a small sample of the material.

B. Input the geometry of the sample insulator into the program to compute the form factor, thus calculating the conductivity.

C. Find the linear relationship between the conductivity and the ESDD value; represent it using mathematical equations; and input it into the program.

Step 2: Obtain the electric field distribution under different surface conditions by conducting simulation with material, insulator shape and surface condition information as inputs to the Coulomb software. Represent the Coulomb output by an equation; input it into the Matlab program.

Step 3: Input the geometry of the target insulator design and the supply voltage to the Matlab program in order to get the predicted flashover ESDD value of the typical insulator design with the typical material type under certain voltage supply.

5.2 Role of shape

More simulations were conducted to investigate the effect of insulator shapes on the flashover ESDD. The results are shown in the following sections.

5.2.1 Insulators with different leakage distances

5.2.1.1 Post type insulator

The simulation was conducted for the standard 15 kV (L-G) post type insulator (see Figure 13) assuming the material is EPDM. The 15 kV post type insulator consists of 5 big sheds and 5 small sheds. With 15 kV as supply voltage, by reducing the number of sheds thereby reducing the leakage distance, it is shown that the ESDD value that the insulator can withstand without flashover is reduced.

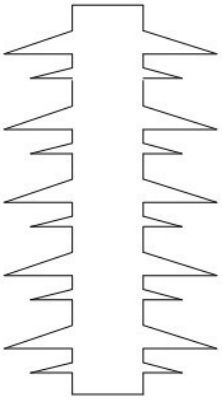

Figure 13.Schematic of standard 15 kV post type insulator

Table 8.The relation between the leakage distance and the number of sheds for post type insulator

Leakage distance (cm)	Number of big sheds	Number of small sheds
49	3	3
63	4	4
77	5	5
90	6	6

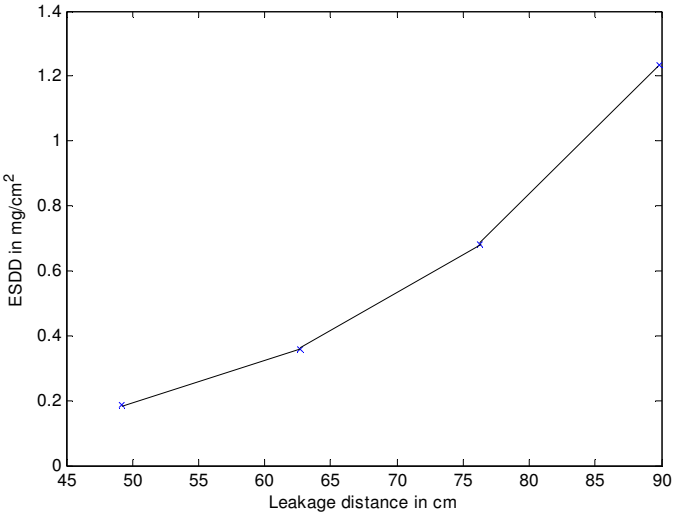

Figure14.Simulation results for post type insulators with different leakage distances (voltage supply: 15 kV)

Simulation was then conducted with the supply voltage increasing to 22 kV. It is seen that the pollution level the post type insulator can withstand decreases.

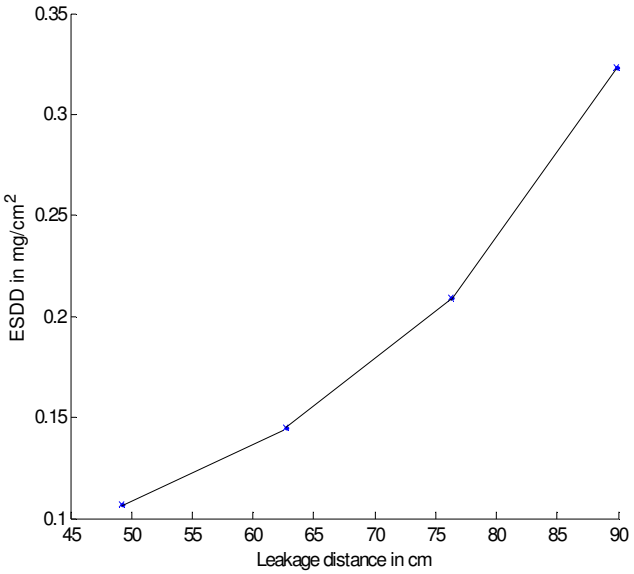

Figure15.Simulation results for post type insulators with different leakage distances (voltage supply: 22 kV)

5.2.1.2 Pin type insulator

The simulation was also conducted for the standard 10 kV (L-G) pin type porcelain insulator. Under a voltage supply of 10 kV, by reducing the number of sheds, it is shown that the ESDD value that the pin insulator can withstand without flashover is reduced. The 10 kV pin type insulator consists of 2 big sheds and 2 small sheds.

Figure 16.Schematic of standard 10 kV pin type insulator

Table 9.The relation between the leakage distance and the number of sheds for pin type insulator

Leakage distance (cm)	Number of big sheds	Number of small sheds
29	1	1
44	2	2
59	3	3

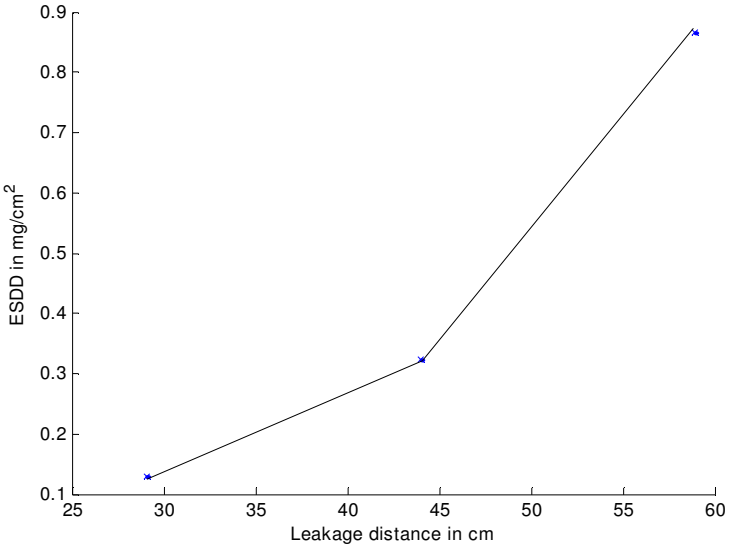

Figure17.Simulation results for pin type insulators with different leakage distances (voltage supply: 10 kV)

Simulation was then conducted with the supply voltage increasing to 15 kV. It is seen that the pollution level the pin type insulator can withstand decreases.

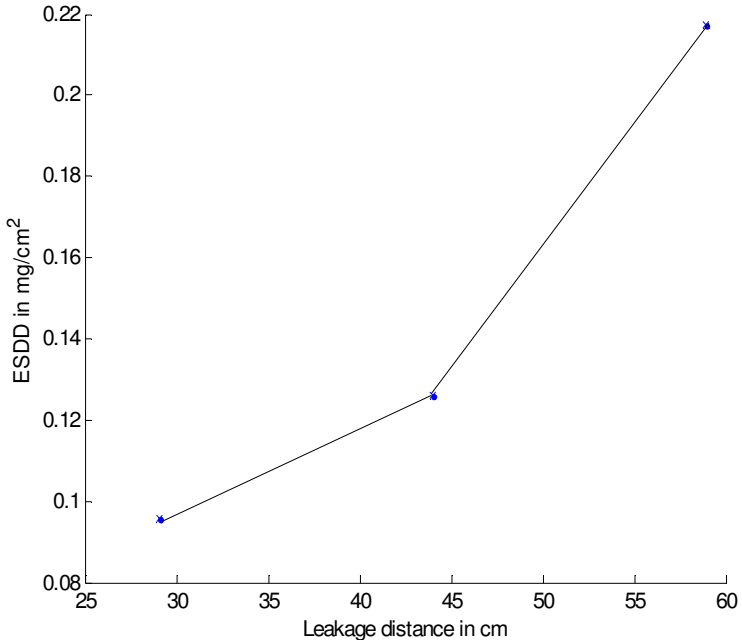

Figure18.Simulation result for pin type insulator with different leakage distance (Voltage supply: 15 kV)

5.2.2 Insulators with different diameters

5.2.2.1 Insulator A and B

Suppose there are two insulators A and B. A is the standard Post insulator for 15 kV. B has the same leakage distance as A, but the diameter of B is twice that of A (In this case the height of B is less than A, the number of sheds is also less than A). Schematics of A and B are shown in Figure 19. The material of the insulators was assumed to be EPDM.

Insulator A with diameter D

Insulator B with diameter 2D

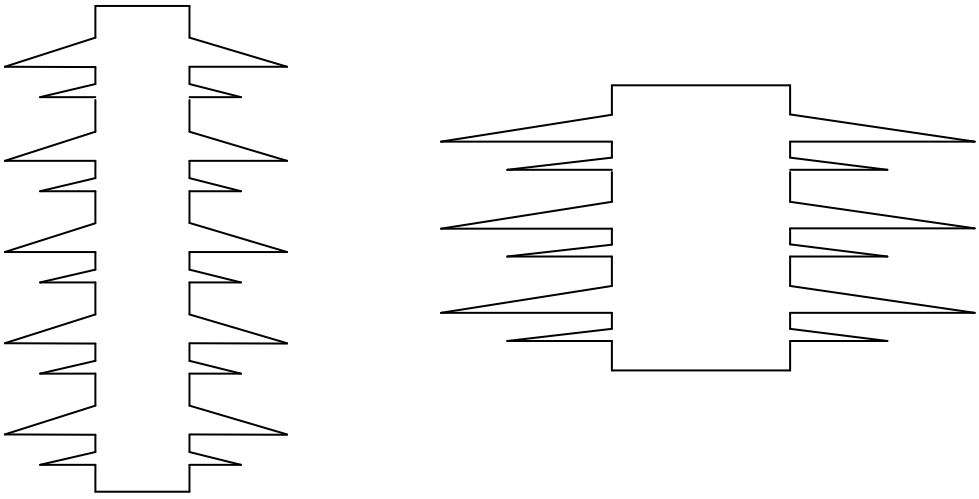

Figure19.Schematics of insulator A and B

With 15 kV applied to the insulator, the leakage distance is changed by changing the number of sheds. In Figure 20, the upper curve is the simulation result for Insulator A and the lower curve is the simulation result for Insulator B. It can be seen that while A and B have the same leakage distance, the pollution severity that B can withstand is lower that A.

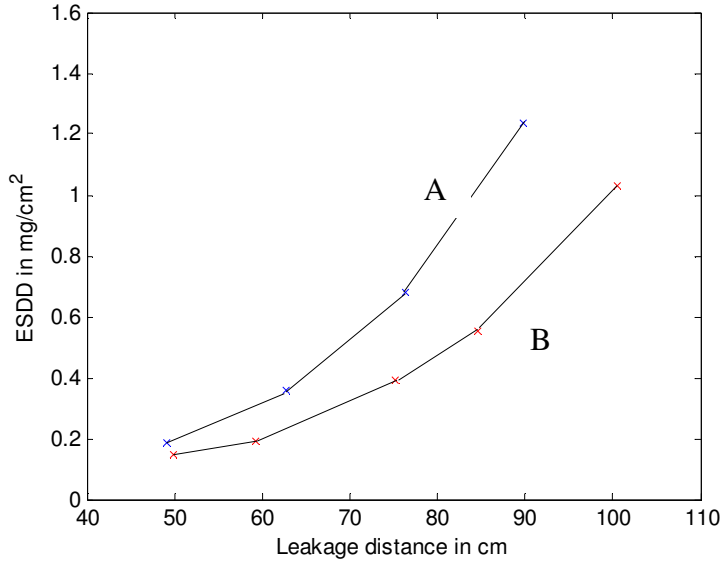

Figure 20.Simulation results for insulator A and B

5.2.2.2 Post type insulator and instrument transformer

C is the standard Post insulator. D is the instrument transformer. It has the same leakage distance (76 cm) as insulator C but the diameter of lower part of D is three times of C. The material of the insulators was assumed to be EPDM. The schematics of C and D are shown below:

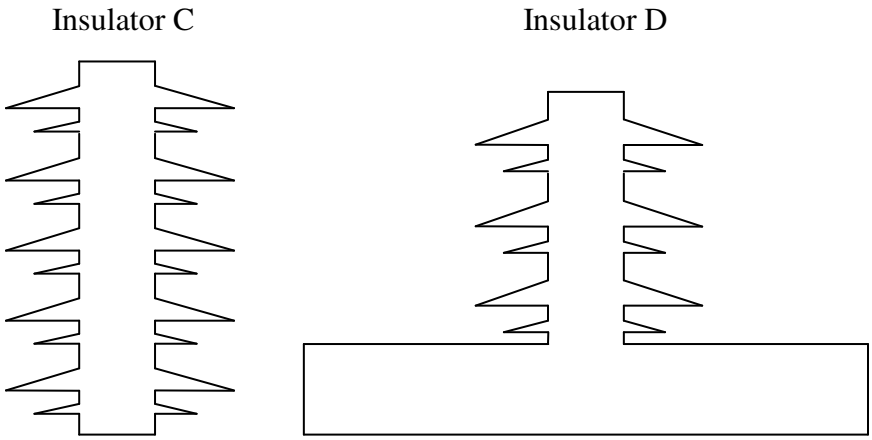

Figure 21.Schematics of insulator C and D

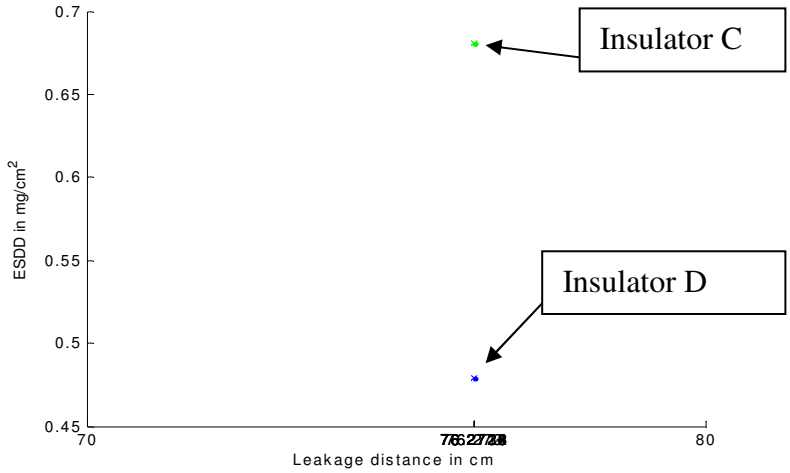

Figure 22.Simulation results of insulator C and D

Applying 15 kV to the insulators, the upper point is the simulation result for insulator C and the lower point is the simulation result for insulator D. It is seen that the pollution severity D can withstand is much lower than C.

5.2.3 Insulators with different shed spacing

Due to the formation of dry bands on the thin part of an insulator, the shed spacing could affect the performance of the insulator. Simulation was conducted on two insulators with different shed spacing as shown in Figure 23. The material of the insulators was assumed to be EPDM. All other aspects of the insulators were assumed to be identical. The details of the insulators are shown in Table 10:

Table 10.Details of the two insulators with different spacing

Insulator	Leakage distance (cm)	Shed diameter (cm)	Shed spacing (cm)	Core shaft diameter (cm)
1	77	12	1.4	4.5
2	77	12	5.2	4.5

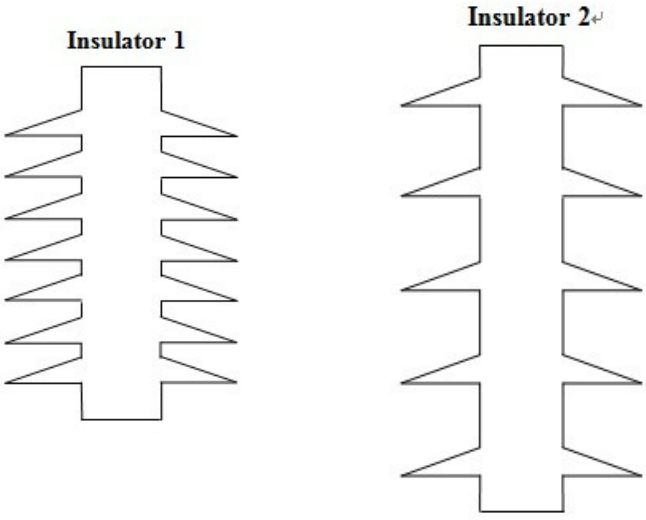

Figure 23.Schematics of the two insulators with same leakage distance but different shapes

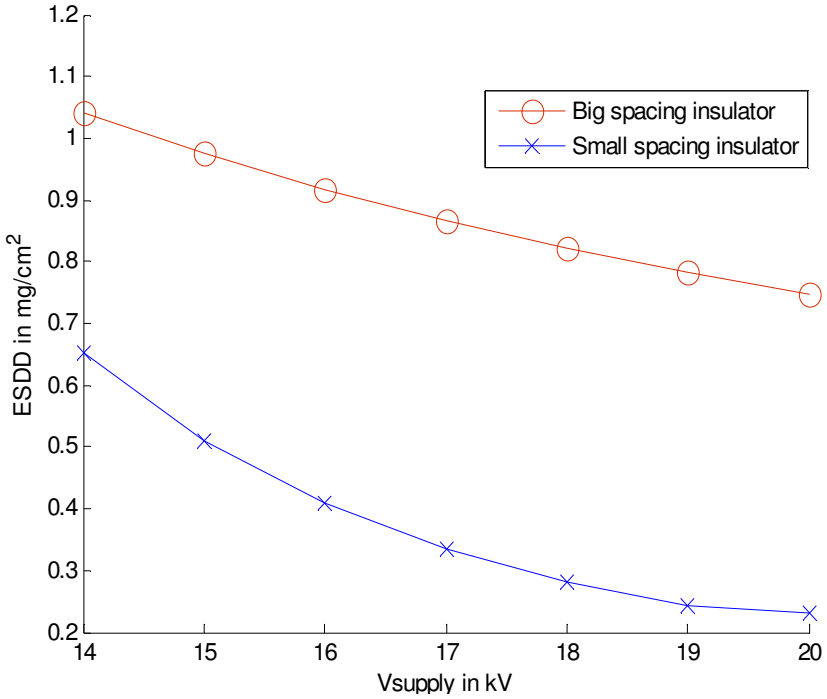

Figure 24.Simulation results for the two insulators

Figure 24 shows that the insulator with big spacing has much better performance than insulator with small spacing. This is because the big spacing insulator allows a longer dry band on the shank. It is harder for the arc to bridge the long dry band and flash over, thus it requires more pollution for the big spacing insulator to flashover.

5.2.4 Insulators with different diameters and spacing

Simulation was conducted on three insulator designs shown in Figure 25. The housing material was assumed the same (EPDM) in all insulators. The leakage distances of the three insulators were also assumed to be the same. The geometrical details of the insulators are shown in Table 11.

Table 11.Details of the three insulators

Type of insulator	Leakage distance (cm)	Shed diameter (cm)	Shed spacing (cm)	Shank diameter (cm)
Post	77	15.5	1.2	6.8
Pin	77	16/11.5	1.4	7.8
Suspension	77	12.5	3.7	2.2

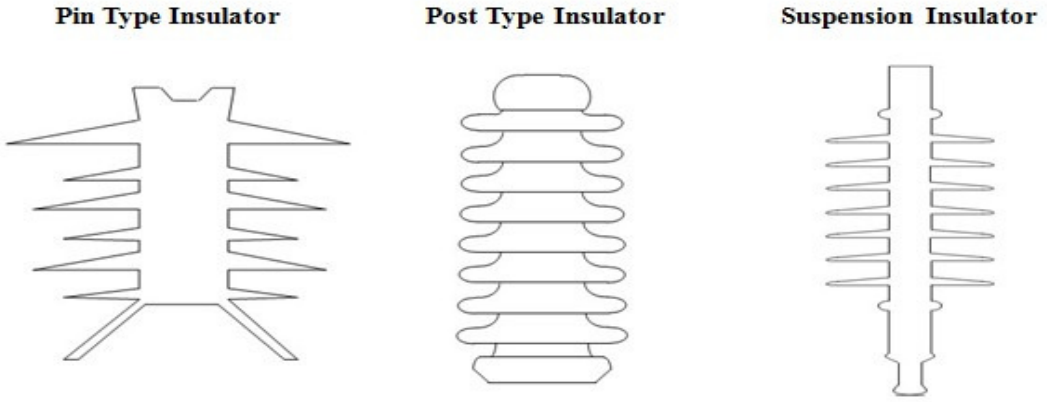

Figure 25.Schematics of the three insulators modeled with same leakage distance and housing material

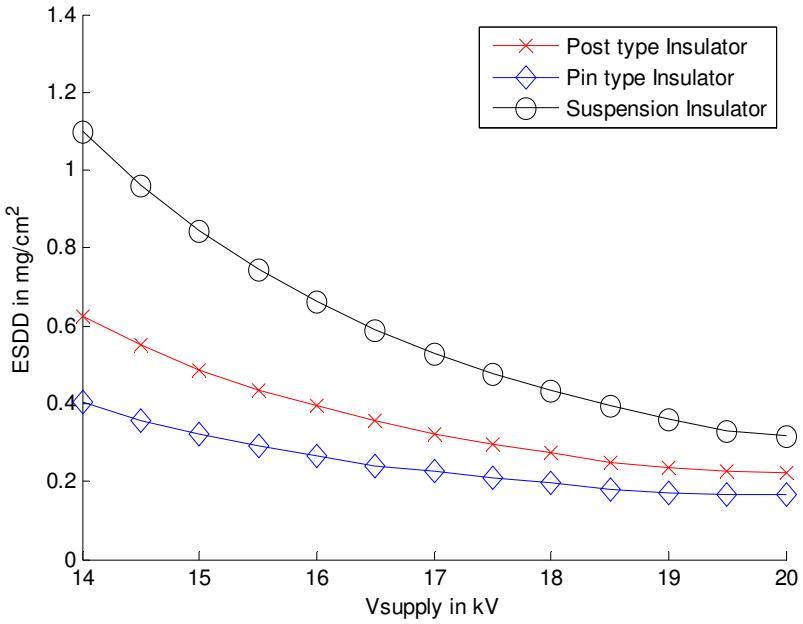

Figure 26.Simulation results for the three insulator types

Figure 26 shows the results of the calculations. It is shown that if the material, leakage distance and voltage are fixed, the suspension insulator design has best performance followed by the post and then the pin type designs.

5.3 Insulators with different materials and shapes

Simulation was also conducted to compare insulators (E and F) with different materials and dimensions. The details of the insulators simulated are shown in Figure 27 and Table 12.

Table 12. Details of the two insulators with different materials and dimensions

Type	Material	Number of big shed	Number of small shed	Leakage distance (cm)
Post (E)	EPDM	5	5	77
Post (F)	Silicone rubber	3	3	49

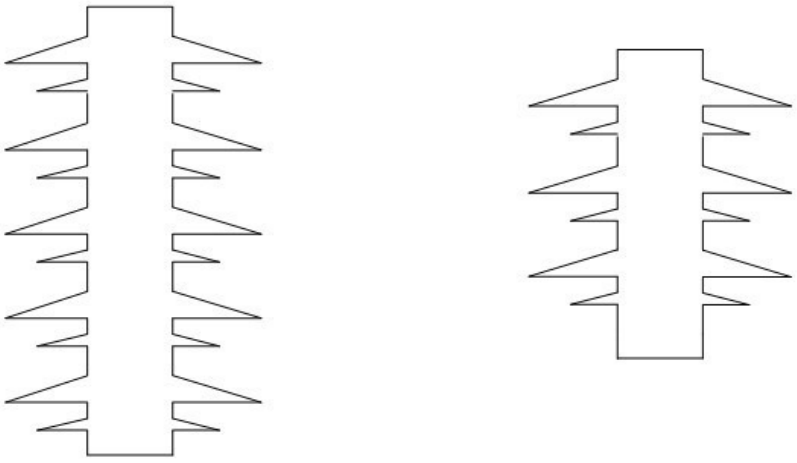

E F

Figure 27.Schematics of insulator E and F

Figure 28 shows that the flashover performance of a silicone rubber insulator with 3 big and small sheds is better than the EPDM insulator with 5 big and small sheds. This is assuming that the silicone rubber remains hydrophobic and the EPDM rubber remains hydrophilic. In practice it is normal to keep the clearances (or the connection length) the same, irrespective of the insulator type used. If the silicone rubber insulator shown in Figure 27 were to be of the same height as the EPDM insulator, then its performance would be even better than shown in Figure 28 due to the larger spacing between the sheds. This could possibly help the insulator manufacturer to make economic and secure choices when they select the insulator material and design.

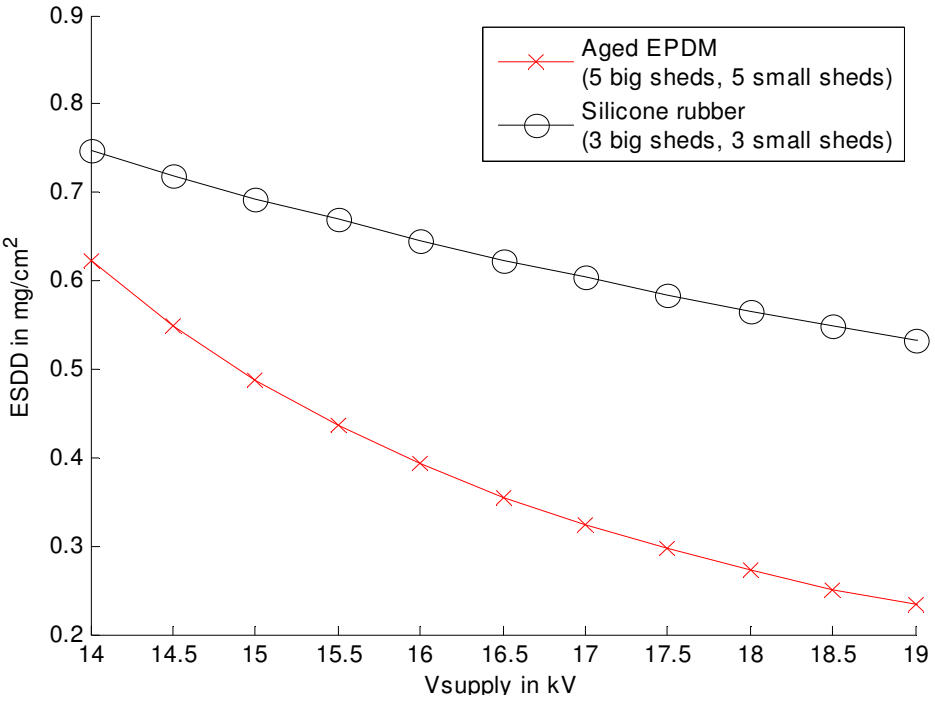

Figure 28.Simulation results for insulator E and F

CHAPTER 6

CONCLUSION

This report presents a model that can determine the pollution severity (in terms of ESDD) at which flashover occurs with a given system voltage for various types of practical insulator configurations. The model makes some improvements over existing models such as introducing the dry band formation and considering the insulator material effects on the pollution flashover. The report starts with an introduction of the pollution flashover problem and a literature review of the existing flashover models. The problems with the existing models are then pointed out. There is a detailed discussion about the proposed model algorithm and the simulation steps. Simulations were conducted using the new program for different insulator designs and materials to validate the model. The results show good agreement with experimental results and engineering judgment.

Still, in the area of flashover modeling, there are many interesting aspects that are worth exploring in the future, including

1. The effect of the power source strength on the pollution flashover performance of insulators. The power source in the lab is not as strong as in the field. There is a situation in the field where a strong power source might "push" the arc from one shed to another shed, which is rarely seen in the lab with the weak power source. Some researchers have published papers on this topic [17, 33, 34], but the real principle behind it is still unknown.
2. The determination of the arc constants. As for now, most of the researchers

obtain the arc constants by fitting the model with the experiment results. These constants could vary largely and the value is mostly unpredictable. It would be helpful if more studies and experiments are done to obtain a generalized standard that can help determine the arc constants based on the material, voltage level or other aspects.

3. For now, the data used in the program is largely based on lab measurements of ESDD and resistance, the value of which could vary for different lab situations. It would be helpful if a more generalized term that will not change much with the lab situations can be found to quantify the surface situation of an insulator
4. The electric field distribution curve obtained from Coulomb was employed in the Matlab program for this study. The combination of electric field simulation and numerical calculation for a pollution flashover study would be an interesting area to be further explored.

REFERENCE

[1] J. S. T. Looms, “Insulators for high voltages”, Peter Peregrinus Ltd., London, U. K, 1988.

[2] J. P. Holtzhausen, “A critical evaluation of AC pollution flashover models for HV insulators having hydrophilic surfaces”, Ph.D. Dissertation, The University of Stellenbosch, 1997.

[3] “IEEE Std 4-1995, IEEE standard techniques for high-voltage testing”, Power Engineering Society, 1995.

[4] R. S. Gorur, E. A. Cherney and J. T. Burnham, “Outdoor Insulators”, Ravi S. Gorur Inc., phoenix, Arizona, USA, 1999.

[5] R. Lings, V. Chartier and P. S. Maruvada, “Overview of transmission lines above 700 kV,” IEEE PES Conference and Exposition in Africa, pp. 33-43, 2005.

[6] B. F. Hampton, "Flashover mechanism of polluted insulation", Proceedings of the Institution of Electrical Engineers, Vol.111, No.5, pp.985-990, 1964.

[7] E. C. Salthouse, "Initiation of dry bands on polluted insulation," , Proceedings of the Institution of Electrical Engineers , Vol.115, No.11, pp.1707-1712, 1968

[8] A. Al -Baghdadi, “The Mechanism of Flashover of Polluted Insulation,” Ph.D. Dissertation, The Victoria University of Manchester, 1970.

[9] T. C. Cheng, “Mechanisms of Flashover of Contaminated Insulators”, Doctoral Thesis, Department of Electrical Engineering, MIT, 1974.

[10] J. A. R. Hernanz, J.J.C. Campayo, J. M. Gogeascoechea, I.Z. Belver, “In sulator pollution in transmission lines”, Departamento de Ingeniería Eléctrica Escuela Universitaria de Ingeniería

[11] H. Sedigh Nezhad, A.Gholami, A.Jalilian, M.T.Hassanzadeh, “ Performance improvement of insulator string in polluted conditions”, http://lutung.lib.ums.ac.id/dokumen/ebooks/Elektro/jes/journal.esrgroups.org/jes/papers/4_3_8.pdf

[12] Working Group 04 of Study Committee No. 33, “A critical comparison of artificial pollution test methods for HV insulators”, Electra, pp.117-136, 1979.

[13] F. A. M. Rizk, “Mathematical Models for Pollution Flashover”, Electra, Vol.78, pp.71-103, 1981.

[14] L. L. Alston, “Growth of discharges on polluted insulation”. Proceedings of the Institution of Electrical Engineers, Vol.110, No. 7, pp.1260-1266, 1963.

[15] B. F. Hampton, “Flashover mechanism of polluted insulation”, Proceedings of the Institution of Electrical Engineers, Vol.131, No. 4, 1964

[16] S. Hesketh, “General criterion for the prediction of pollution flashover”, Proceedings of the Institution of Electrical Engineers, Vol.114, no 4, pp.531-532, 1967

[17] R. Matsuoka, T. Usui, Y. Hayashi, S. Ito, K. Kondo, “Influence of power source on contamination withstand voltage of polymer insulators”, Eleventh International Symposium on High Voltage Engineering, Vol.4, pp.276-279, 1999.

[18] H. H. Woodson, A.J. McElroy, “Insulators with contaminated surfaces, part III: modeling of discharge mechanisms”, IEEE Transaction on Power Apparatus and Systems, Vol.89, No.8, pp.1868-1876, 1970.

[19] F. A. M. Rizk, “Application of dimensional analysis to flashover characteristic of polluted insulators”, Proceedings of the Institution of Electrical Engineers, Vol.117, No. 12, 1970.

[20] P. Claverie, “Predetermination of the behavior of polluted insulators”, IEEE Transaction on Power Apparatus and Systems, Vol.90, pp.1902 -1924, 1971.

[21] P. Claverie, Y. Porcheron, “How to choose insulators in polluted areas”, IEEE Transaction on Power Apparatus and Systems, Vol.92, pp.1121-1131, 1973.

[22] X. Zhang, S.M. Rowland, "Behavior of low current discharges between water drops”, IEEE Conference on Electrical Insulation and Dielectric Phenomena, pp.437-440, 2009.

[23] D. L. Williams, A. Haddad, A.R. Rowlands, H.M. Young, R.T. Waters, "Formation and characterization of dry bands in clean fog on polluted insulators", IEEE Transactions on Dielectrics and Electrical Insulation, Vol.6, No. 5, pp.724-731, 1999.

[24] IEC 815, “Guide for the selection of insulators in respect of polluted conditions”, 1986

[25] K. Shenoi, R. S. Gorur, "Evaluating station post insulator performance from electric field calculations," IEEE Transactions on Dielectrics and Electrical Insulation, Vol.15, No.6, pp.1731-1738, 2008

[26] IEEE “Standard techniques for high-voltage testing”, IEEE Std 4. 1989.

[27] H. El-Kishky, R.S. Gorur, "Electric potential and field computation along AC HV insulators", IEEE Transactions on Dielectrics and Electrical Insulation, Vol.1, No.6, pp.982-990, 1994.

[28] C. Texier, B. Kouadri, "Model of the formation of a dry band on a NaCl-polluted insulation", Proceedings of the Institution of Electrical Engineers, Vol.133, No.5, pp.285-290, 1986.

[29] "COULOMB 8.0 Users and technical manual, Integrated Engineering Software, 2010.

[30] A. de la O, R.S. Gorur, J.T. Burnham, "Electrical performance of non-ceramic insulators in artificial contamination tests. Role of resting time," IEEE Transactions on Dielectrics and Electrical Insulation, Vol.3, No.6, pp.827-835, 1996.

[31] R. S. Gorur, H. M. Schneider, J. Cartwright, Y. Beausajour, K. Kondo, S. Gubanski, R. Hartings, M. Shah, J. McBride, C. de Tourreil and Z. Szilagyi", IEEE Transactions on Power Delivery, Vol.16, No. 4, pp.801-805, 2001.

[32] S. Venkataraman, R.S. Gorur, "Extending the applicability of insulator flashover models by regression analysis", IEEE Transactions on Dielectrics and Electrical Insulation, Vol.14, No.2, pp.368-374, 2006.

[33] F.A.M. Rizk, D.H. Nguyen, "Digital simulation of source-insulator interaction in HVDC pollution tests", IEEE Transactions on Power Delivery, Vol.3, No.1, pp.405- 410, 1988.

[34] F.A.M. Rizk, M. Bourdages, "Influence of AC source parameters on flashover characteristics of polluted insulators", IEEE Power Engineering Review, Vol. PER-5, No.4, pp.51, 1985.

APPENDIX A

FORM FACTOR CALCULATION

The form factor calculation is complicated, but the basic idea is the equation below:

$$form\_factor = \int_0^L [1/p(l)]dl$$

Where:

$p(l)=\pi * D$: the circumference at partial creepage distance l (D is the diameter)

dl: the increment of integration

L: the total creepage distance

Below is some explanation about form factor from IEEE Standards:

"The form factor is determined from the insulator dimensions and may be estimated graphically by plotting the reciprocal value of the insulator circumference against the partial creepage distance up to the point reckoned; the area under this curve gives the form factor."[3]

Because the insulator is not a simple cylinder, diameter D varies along the creepage distance. In order to make it easier to understand how the form factor is calculated, an example is used. Suppose we have an insulator shown in Figure 29 with leakage distance:

$$L= a+c+d+f+g+k+j+i+h$$

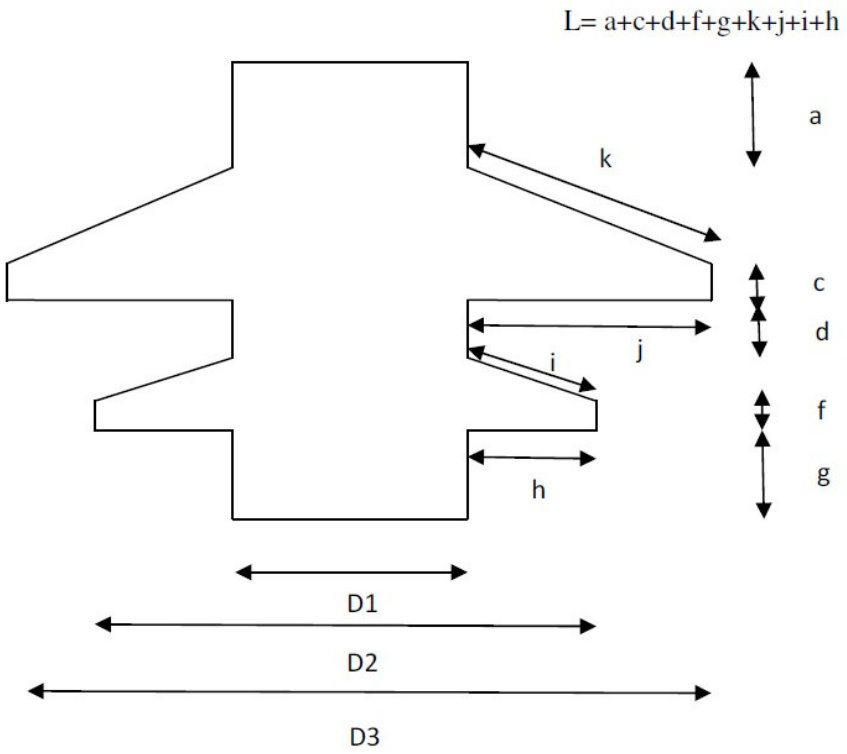

Figure 29. Example of insulator for form factor calculation

Given arc length *x*, the remaining creepage distance will be *L-x*, let *y=L-x*

When $0<y<g$, $D=D1$, $\frac{1}{p(l)} = 1/(\pi * D1)$

When $g<y<g+h$, $D=D1+(y-g)*2$, $\frac{1}{p(l)} = 1/(\pi * (D1 + (y-g) * 2)$

When $g+h<y<g+h+f$, $D=D2$

When $g+h+f<y<g+h+f+i$, $D=D2-(y-g-h-f)*cos(shed\ angle)*2$

When $g+h+f+i<y< g+h+f+i+d$, $D=D1$

When $g+h+f+i+d<y< g+h+f+i+d+j$, $D=D1+(y- g-h-f-i-d)*2$

When $g+h+f+i+d+j <y< g+h+f+i+d+j+c$, $D=D3$

When $g+h+f+i+d+j+c <y < g+h+f+i+d+j+c+k$, $D= D2-(y- g-h-f-i-d-j-c)*cos(shed\ angle)*2$

When $g+h+f+i+d+j+c+k<y< g+h+f+i+d+j+c+k+a$ $D=D1$

If plotting the *1/p(l)* vesus *y*, the figure will look like to the curve below:

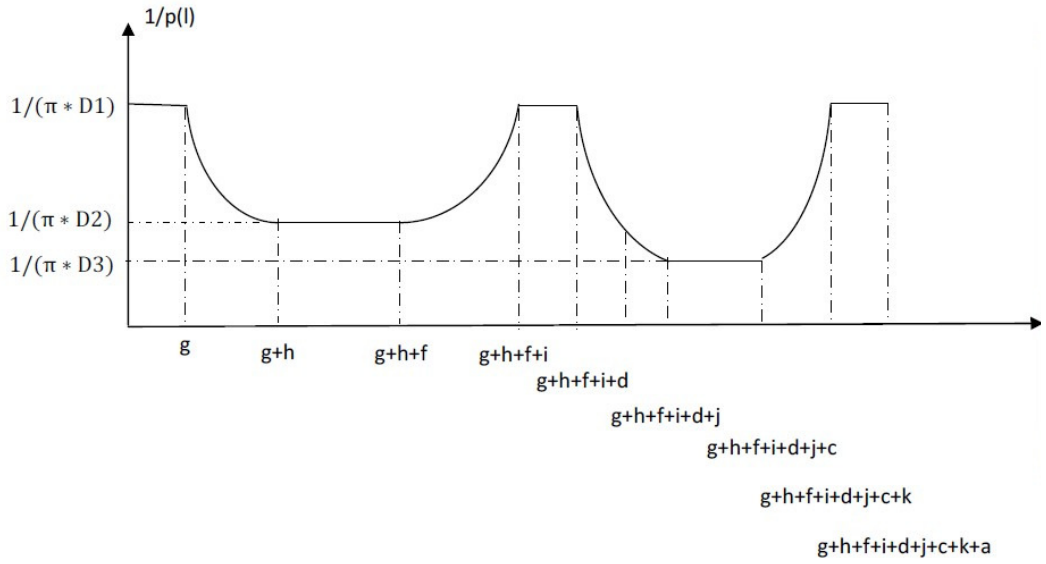

Figure 30. Curve for form factor distribution

With given *L* and *x*, the program will know where *(L-x)* is located on the curve. Then it will integrate *1/p(l)* to get the value of the area under the curve, thus getting the form factor value for *(L-x)*. The value of area in the shadow is the form factor regarding current leakage distance *(L-x)*.

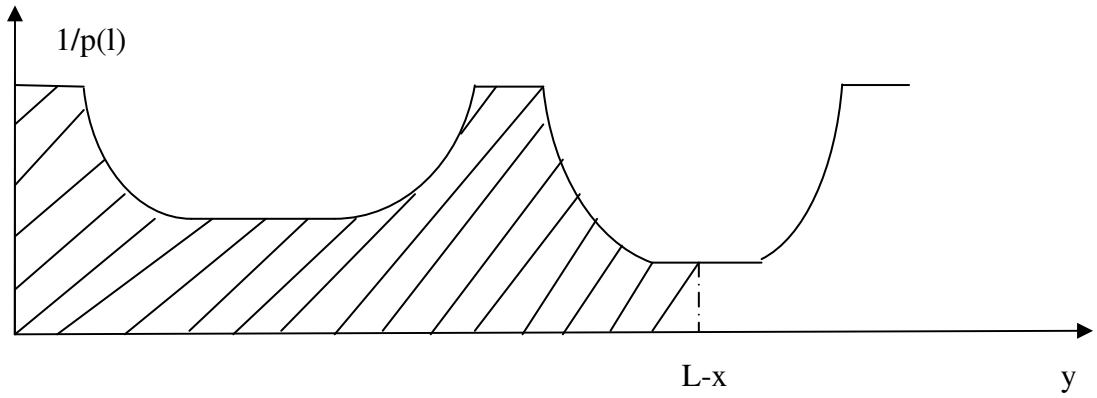

Figure 31. The shadow area showing the form factor value